Title: Symmetric and Asymmetric Causal Neural Firing Interactions across Striatum, Anterior Cingulate and Prefrontal Cortex during Cognitive Control

William H Alexander[1,2,3*], Thilo Womelsdorf[4,5]

[1]*Center for Complex Systems & Brain Sciences, Florida Atlantic University, Boca Raton, USA*
[2]*Department of Psychology, Florida Atlantic University, Boca Raton, USA*
[3]*The Brain Institute, Florida Atlantic University, Boca Raton, USA*
[4]*Department of Psychology, Vanderbilt University, Nashville, TN 37240.*
[5]*Department of Biomedical Engineering, Vanderbilt University, Nashville, TN 37240.*

***Corresponding Author:** walexander@fau.edu

Keywords:

Feature-based attention, granger causality, cognitive control, hierarchical reinforcement learning

Abstract:

Generally, successful performance of complex cognitive tasks depends on the function of interacting regions, including anterior cingulate cortex (ACC), lateral prefrontal cortex (LPFC) and ventral striatum (VS). During task performance, markers of communication amongst regions in the cognitive control network are frequently observed. Typically, however, these markers are agnostic with respect to the direction in which information passes through the system – although firing rate correlations and enhanced synchrony between regions are suggestive of causal interactions, these approaches are not sufficient for determining the influence of on region on another. In this manuscript, we apply a novel approach to investigate the causal dynamics of regions in the cognitive control network during correct and incorrect performance. Using experiment-averaged time courses recorded from ACC, LPFC, and VS, we identify neurons within each region exhibiting task-sensitive response dynamics and calculate Granger causality for each pair of neurons during salient task events. Cluster analysis of causality time courses identifies significant, bidirectional causality between regions following stimulus and feedback onset.

Introduction

Adaptive behavior is brought about by an interplay of multiple brain areas. During reward-based learning this interplay involves correlations of spiking activity and coherent local field potential activity in the anterior cingulate cortex (ACC), the lateral prefrontal cortex (LPFC), and their partly overlapping convergent target regions in the anterior striatum (STR). A rich set of studies have shown that these three brain areas show functionally correlated activity when a reward predictive cue is processed (Womelsdorf et al., 2014; Oemisch et al., 2015; Voloh et al., 2018), and when the feedback of a choice gives rise to a reward prediction error (Rothe et al., 2011; Antzoulatos & Miller, 2014; Voloh et al., 2020). However, it has remained unresolved whether functional activity correlations indicate the direction neuronal information flow. Such a systematic information flow is predicted by hierarchical models of cognitive control (Frank & Badre, 2012; Alexander & Brown. 2015). For example, the hierarchical error representation model (HER model) succeeds to reproduce complex behavioral adaptation by assuming cue and context specific representations at higher representational levels that biases the information processing at lower brain areas during top-down guided choices, while the processing of choice outcomes trigger computational sequences that travel in the reverse direction in order to arrive at prediction errors for improving future predictions (Alexander & Womelsdorf, 2018). According to these computational frameworks the cue- and outcome- specific processing should be reflected in directional information flow.

To measure directional information transfer it is paramount to have high temporal resolution to capture transient 50-200 ms long occurrences of neural events that are indicative of directional synaptic influences between sending and receiving brain areas (Palmigiano et al., 2017; Oemisch et al., 2015; Luczak et l., 2015; Luz; Shin et al., 2017; Lundquist et al., 2018). Trial-by-trial correlations of action potential sequences and spike-spike cross-correlation approaches are, however, highly variable and of marginal strength even for anatomically connected anterior cingulate and lateral prefrontal cortices (Oemisch et al., 2015). An alternative means to index directionality is the calculation of phase delays during period of phase-synchrony of spikes and local field potentials (LFP's) (Womelsdorf et al., 2014; Voloh et al., 2018; Voloh et al., 2020; Antzoulatos et al., 2014). However, local field potentials reflect not only how synaptic events from a remote, afferent source modulates a local area but inevitably also reflect local sources from neighboring neurons. Such a synaptic mixture of local and remote synaptic influences makes it ambiguous to interpret phase specific directional transfer and gives rise to spurious directional indices in the absence of true synaptic drive of a sending to a receiving area (Schneider et al., 2020). To prevent the difficulties interpreting field potential effects it is therefore desired to quantify directional exchange of information directly from neuronal spiketrain interactions.

Here, we establish a neuronal spike-envelope technique to estimate the net direction and strength of interareal activity modulation. To this end we assume that the average spiking envelope of a neuron around behaviorally significant events provides a fair dynamic description of its overall task involvement. Based on this assertion we then quantify how the temporal activity profile of a neuron predicts the temporal activity profile of an independently recorded neuron. Using classical Granger causality metrics we statistically determine the existence of a Granger causal neuronal

interaction of a sending and receiving neuron when the activity profile of the receiver is better predicted by the activity profile of the sending neuron than by its own past activity profile. Next we assemble the Granger causal spiking envelope for pairs of brain areas and use clustering analysis to identify reliable Granger-causal time courses for this specific brain area. Using this approach, we show that robust Granger-causal time courses exist for neurons recorded in anterior cingulate cortex (ACC), lateral prefrontal cortex (LPFC) and Striatum (STR). We show that groups of neurons in these brain areas engage in significant bidirectional granger causal spiketrain interactions during the processing of reward-predictive cues and during the processing of outcomes. We speculate that these directionally linked neuronal clusters could be the candidate units that realize ordered information transfer as predicted by hierarchical cognitive control models.

Results

We analyzed neuronal activity from single neurons in ACC, LPFC and Striatum from two rhesus monkeys performing a feature-based reversal learning task (Oemisch et al., 2019). During this task the animals processed covertly, without moving their eyes the onset of two peripheral colors in order shift attention to one over the other stimulus. After making a saccadic choice about a transient luminance. Change of the attended stimulus the animals received liquid reward for correct trials. The animals had to learn without explicit cue which stimulus color was associated with reward over ≥30 trials through trial-and-error (see Materials and Methods). We focused our analysis around the onset of the color cue whose reward prediction the animals had to learn, and around the time of the outcome that signalled either correct or incorrect trial outcomes and thus triggered the evaualtion of prediction errors.

Cue Period

During correct trials (**Fig. 1**), our analyses identified an overall increase above chance in measures of causality amongst all three regions: activity in clusters of neurons in each region Granger-causes neural activity in each of the other regions. This finding is consistent with cue-specific, transient increases of spiketrain correlations (Oemisch et al., 2015), and phase synchronization of spikes and local field potentials (Voloh et al., 2018, 2020; Antzoulatos & Miller, 2014; Rothe et al., 2011) between ACC, LPFC, and Striatum. This suggests that, following the occurrence of an event requiring a response, correct behavior depends on the recurrent interplay amongst task-sensitive neurons across the medial and lateral anterior fronto-striatal networks.

In contrast, this tight coupling of regions is not observed when considering neurons that are less sensitive to task demands (**Fig. 1**), or during trials in which behavioral errors are committed (**Fig. 1**). In the case of 'task-insensitive' neurons (operationalized as neurons with lower relative variance), we still observe above-chance causal measures, but these tend to be unidirectional. This effect is particularly obvious for ACC-VS and LPFC-VS interactions before and after cue presentation. In both cases, activity in VS is granger-caused by activity in ACC or VLPFC (**Fig. 1**). Notably, and in contrast to the pattern observed for task-sensitive neurons, this 'top-down' flow of information from cortex to striatum peaks around the time of cue presentation, after which

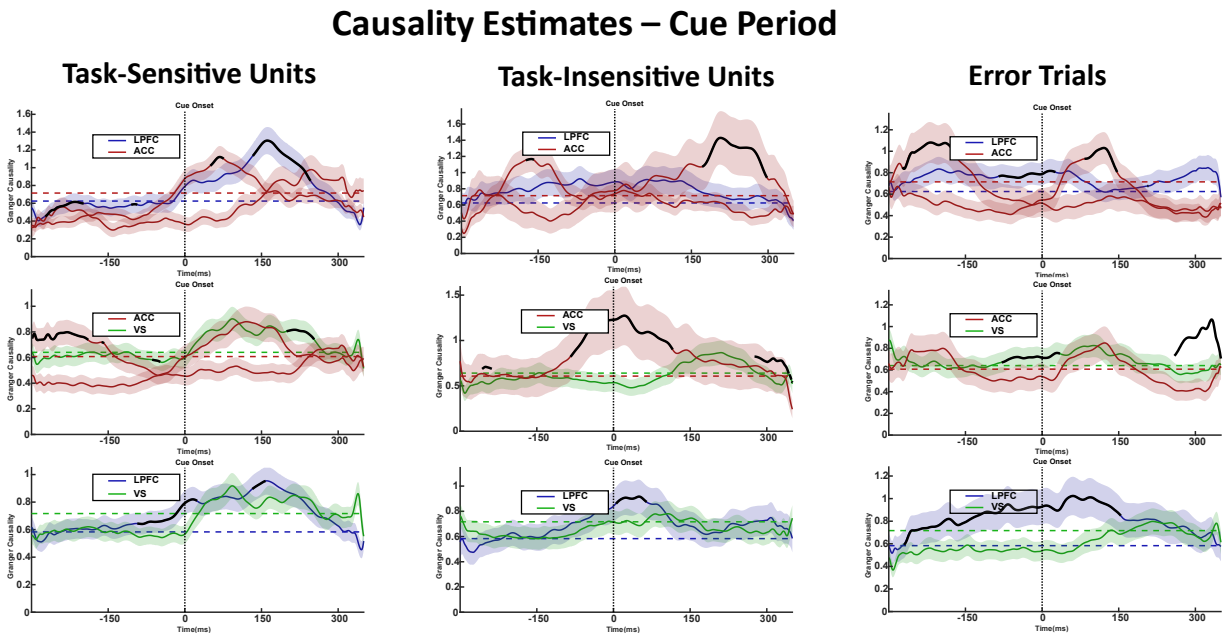

Figure 1 – Causality during correct and error trials at cue presentation. We identified clusters of neuron pairs in the cognitive control network exhibiting significant bidirectional causality following cue presentation (Left Panels). Although the net directionality was higher for one region than the other in some cases (thick black lines), causal measures from both regions were significantly above chance ($p<0.001$, FWE corrected, dashed horizontal lines). Analysis of 'task-insensitive' units (Center Panels) also identifies significant causal clusters. In contrast to clusters identified for task-sensitive units, task-insensitive causality is not locked to stimulus onset, and is more strongly unidirectional in nature. During Error Trials (Right Panels), causality measures for task-sensitive units are noticeably attenuated, and do not demonstrate the same degree of bidirectional coherence observed for correct trials.

it tails off. One possibility is that neurons that are less sensitive to punctate events during a task may carry information regarding the expected timing of events within a task, i.e., rather than responding to events themselves. The directed flow of information is also apparent in ACC-LPFC interactions – here, we observe that task-insensitive neurons in ACC Granger cause activity in LPFC around 200ms after cue onset.

Compared to causality measures for task-insensitive neurons, measures for task-sensitive neurons during error trials were generally weaker overall. That is, while significant unidirectional causality was observed across the fronto-striatal network for task-insensitive neurons during correct trials, trials that ended in a behavioral error lack directional firing interactions altogether within the network. Relative to ACC-LPFC interactions during correct trials, the same clusters during error trials indicated that ACC→LPFC signaling is delayed and fails to elicit recurrent LPFC→ACC signaling. For ACC-VS and LPFC-VS interactions, the pattern of interactions remains similar, but is qualitatively weaker than during correct trials. Generally, the pattern of results observed on error trials following cue presentation suggest an overall break-down in communication and coordination amongst regions in the fronto-striatal network.

Feedback Period

Similar to our observations following cue presentation, causality following feedback presentation on correct trials were marked by above-chance, bi-directional connectivity amongst all regions in

the fronto-striatal network (**Fig. 2**). In contrast to post-cue measures, however, causal measures tended to favor one region over another – i.e., even if two regions significantly causally influenced each other, one region might have a significantly stronger influence, and the direction of this significant difference could shift over time (**Fig. 2**).

This is especially apparent with LPFC interactions with VS and ACC – around 150 ms following reward onset, the causal influence of VS and ACC on LPFC is significantly greater than the influence of LPFC on VS/ACC (**Fig. 2**). In the case of the interaction between LPFC and VS, the direction of the influence shifts at approximately 200ms, with the influence of LPFC on VS significantly greater than the other way around. Causal interactions between ACC and VS are bidirectional symmetrical, although there appears to be a slight shift in net causality from

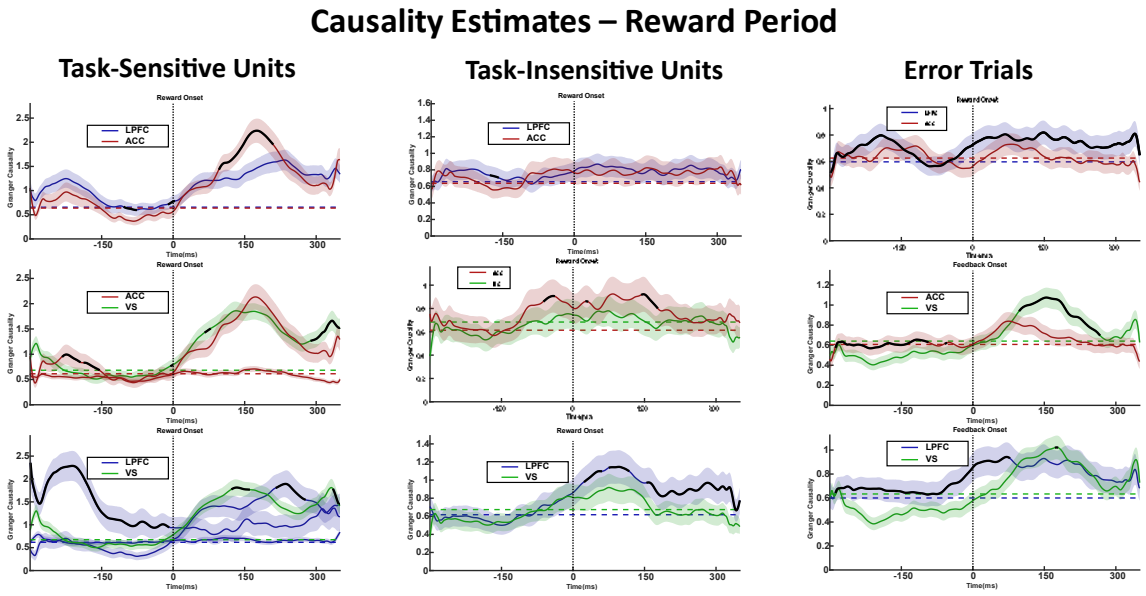

Figure 2 – Causality during correct and error trials at feedback. We identified clusters of neuron pairs in the cognitive control network exhibiting significant bidirectional causality following feedback presentation (Left Panels). As observed following cue presentation, causal measures from both regions were significantly above chance ($p<0.001$, FWE corrected, dashed horizontal lines). Causal measures for task-insensitive units (Center Panels) were qualitatively weaker than for task-sensitive units, although in some cases they did exceed chance level. During error trials (Right Panels), reward was withheld due to incorrect performance. Significant causal clusters, especially in VS, appear more strongly locked to feedback than following cue presentation (cf. Fig 2).

VS→ACC around 75ms to ACC→VS at 150ms.

In contrast to the results following cue presentation (**Fig. 1**), causal measures following feedback for task-insensitive neurons were overall weaker for VS-ACC and ACC-LPFC interactions than for task-sensitive neurons, and did not indicate a substantial directionality in the flow of information (**Fig. 2**). On the other hand, bidirectional causality was observed for task-insensitive neurons in VS and LPFC, with a significantly greater causal influence of LPFC on VS following feedback onset.

On error trials, for which feedback was the withholding of reward, significant bidirectional interactions emerged between VS-ACC and VS-LFPC following the time at which reward would

be delivered on correct trials. In the case of VS-ACC, this bidirectional interaction develops simultaneously at first, with a stronger influence of VS→ACC evident around 150ms (**Fig. 2**). In contrast, there is a significant causal influence of LPFC on VS which begins earlier, preceding feedback onset, and VS→LPFC causality is observed later on, also peaking around 150ms following the time at which feedback would be presented.

Unit Activity

While the causality measures derived above may suggest the direction and possible content of information transmitted between two regions, they do not indicate how neuronal firing changed during the time period of significant directionality. One possibility is that firing increases in one region drive synaptic activity in the target region and increases the likelihood of neural firing in the target population (Schneider et al., 2020). However, synaptic drive of the target area could also target inhibitory cell populations and hence decrease overall firing probability (Medalla et al., 2009; 2017). Alternatively, the directionality of firing rate changes could be due to a third brain area that modulates firing rate increases or decreases of each of the recorded brain areas independently (Qao et al., 2020). These scenarios could underlie the Granger causal modulations albeit with gross variations in overall firing rate modulations during the periods of directional interactions (Schneider et al., 2020).

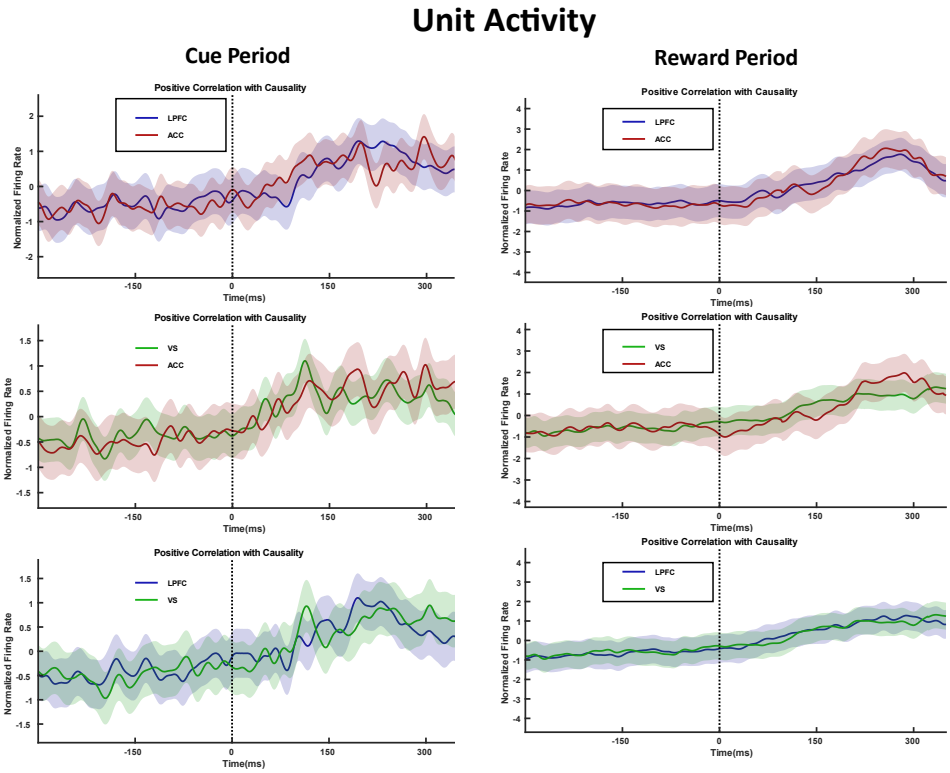

Figure 3 – Unit Activity Correlates with Causality. The averaged activity time course for units associated with significant causality clusters was correlated against causality measures calculated between regions at cue (left panels) and feedback (right panels) periods (positively correlated units shown above). Compared to causality time courses observed in our data, peak firing rates emerged more slowly following task events.

To investigate these possible factors, we analyzed activity for task-sensitive units that were classified as belonging to significant kmeans clusters in our previous analyses (**Fig. 3**). First, for each unit within a significant cluster, we correlated that unit's firing rate with the Granger causality estimate for that region. Units were classified as positively or negatively correlated, or as uncorrelated (non-significant correlation). Unit activity was then standardized, and the average firing rate of units assigned to each class was plotted. This analysis was conducted for each pair of regions (VS-ACC, VS-LPFC, ACC-LPFC) for both the cue onset and feedback onset epochs.

Across all regions, we found that unit firing rate was predominantly positively correlated with Granger causality (**Fig. 4**). Thus, the activity of a unit that participated in a kmeans cluster with significant causal influence on the firing of downstream neuron tended to increase its firing rate. Fewer neurons were negatively correlated, and a marginal number of units involved in a causally-relevant kmeans cluster showed activity that was non-correlated with causality. The upshot is that, in our analyses, causality appeared to be driven primarily, but not exclusively, by increased unit activity.

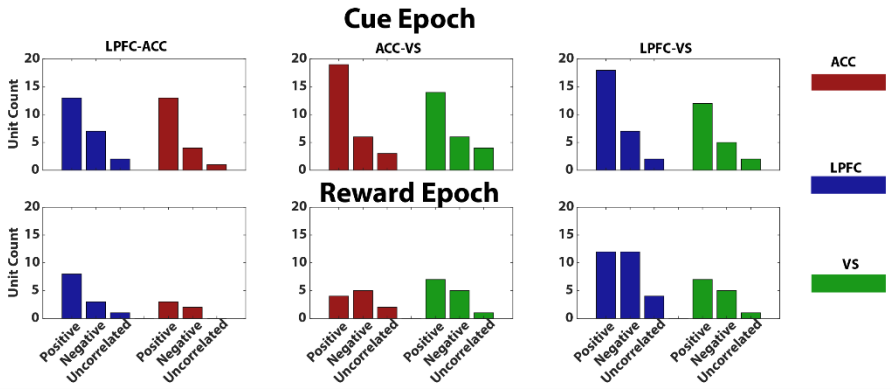

Figure 4 – The majority of units identified as participating in a causal cluster were positively correlated with causality during cue presentation (Top Row), although a significant portion were negatively correlated. The ratio of positively correlated to negatively correlated units decreases during feedback (Bottom Row), although generally positive correlations are more frequently observed than negative correlations.

Discussion

In this manuscript, we describe a new approach for investigating network interactions using single-unit neural data recorded from three major nodes of the anterior fronto-striatal network subserving cognitive control and decision-making. We applied this approach to querying general predictions derived from computational models of prefrontal cortex (W. H. Alexander & Brown, 2015, 2018) based on predictive coding formulations(Rao & Ballard, 1999). These predictions concern the representation of information during cognitive control, how anatomical regions involved in cognitive control and context-depended visual search interact, and how this interaction changes at specific points in the trial, as well as during correct and incorrect performance. Our results are consistent with the functions assigned to ACC, VS, and LPFC by the HER model.

Perhaps least surprising was our observation of a general increase in coupling amongst the regions following cue and reward presentation. Directed pairwise estimates of causality between all regions increased at these points – at least some neurons in each region granger-caused neural activity in each other region. During behavioral performance, especially for complex cognitive tasks, regions in the cognitive control network couple together. Frequently, this coupling is associated with oscillatory synchronization of activity(Marco-Pallares et al., 2008; Rothé et al., 2011; Wang et al., 2016), which has been observed between each of the regions included in this study. One role of the synchronizing oscillatory activity between regions may be to facilitate the transfer of information between them by temporally aligning the disinhibited periods between synchronized neuronal populations (Akam & Kullmann, 2014, Fries, 2015; Hahn et al., 2014; Hahn et al., 2019; Palmigiano et al., 2017; Womelsdorf et al., 2007). In this context, mutual increases in causality estimates between regions can be considered a consequence of more effective communication between those regions – if activity in one region did not have a causal influence on activity in a target region, it could hardly be said to be engaging in communication.

Although causality amongst regions increased generally, we also observed differences in the strength of causal estimates between regions. That is, even if the causal influence of two regions on one another was above chance following a salient event, in some circumstances one region exerted a greater net influence on another. This difference in net causality was most obvious for interactions between dACC and LPFC. Immediately after cue onset, activity in dACC neurons more strongly influenced activity in LPFC neurons (peaking around 75ms), while LPFC more strongly influenced ACC later (peak around 150ms). Following reward and error feedback, in contrast, ACC consistently exerted a stronger influence on LPFC activity. These results directly support predictions of the HER model regarding the development of causal interactions over the course of a trial (Alexander & Womelsdorf, 2018). In the HER model, a brief period of ACC→LPFC causality following cue onset derives from the integration of target and context information: because target information is more directly related to eventual behavioral output, response-related predictions (ACC) evolve more rapidly than context-related activity (LPFC), resulting in an apparent causal interaction relationship. However, because target information alone contains only partial information governing a response, causal interactions later in the trial reflect the influence of context information (LPFC) on identifying and selecting the context-appropriate response (ACC). Conversely, following feedback, the HER model proposes that prediction error signals generated in ACC are used to train error representations in LPFC, resulting in a stronger ACC→LPFC relationship than vice-versa.

Our analyses of 'task-insensitive' neurons identified significant causality components whose time course and network interactions differed qualitatively from 'task-sensitive' neurons. Temporal epochs during which task-insensitive neurons had significant causal influence on target regions did not appear to be locked to the onset of a salient task event such as cue onset or feedback. One possibility is that these neurons reflect tonic maintenance of task information, such as rules and response contingencies that do not typically change from one trial to another, and thus do not vary in firing rate following stimulus or feedback onset within a trial. Furthermore, these neurons exhibited stronger unidirectional effects, rather than the bidirectional causality observed in 'task-sensitive' neurons, especially with respect to 'top-down' effects of cortical sites on VS. Together,

these observations suggest that tonic, task-relevant information maintained in frontal cortex (Sawaguchi & Goldman-Rakic, 1991) may tonically modulate VS function in order to support behavior. VS is frequently associated with information and response gating (O'Reilly & Frank, 2006), often abstracted as a softmax choice function. Cortical afferents to VS may alter parameters of the choice function, such as response temperature or threshold (Parr & Friston, 2017),, which are relatively constant over the course of a single trial.

Causal measures for error trials reflect an interesting dichotomy for cue and reward epochs. Following the presentation of a cue on a trial that will eventually result in behavioral error, causality in the frontostrial network fragments – overall causality estimates for task-sensitive neurons are weaker and, when present, unidirectional. The breakdown of reciprocal interactions in the network may presage the inability to generate correct behavior during response periods. On the other hand, causal measures during the feedback epoch on error trials seem to indicate a 'bottom-up' influence of VS on cortical projection sites. Causal estimates of VS on ACC and LPFC are locked to the time feedback is usually provided (on correct trials), peaking around 150ms in both cases. The VS causal signal may constitute a PE (den Ouden et al., 2010), indicating, in this case, the unexpected absence of the usual rewarding feedback, which is then used to update predictions maintained in frontal cortex.

Comparing experiment-averaged single-unit firing rates to causality estimates suggests that, by and large, increases in neural firing underly causal influences – unit activity tends to correlate positively with causality. However, in each region, we additionally observed units in each region that, while contributing to a causally-significant cluster, displayed activity that was negatively correlated with causal estimates. That is, decreases in unit activity in one region were useful for predicting changes in unit activity (positive or negative) at a projection site. This observation appears broadly consistent with the proportion of excitatory to inhibitory connections observed in cortex (DeFelipe & Fariñas, 1992), suggesting both excitation of neurons in target regions as well as disinhibition of GABA interneurons may contribute to net causality measures between regions.

In this data, unit activity appeared to lag causality measures by around 100ms – for example, peak ACC→LPFC causality following rewards occurred around 150ms, while firing rate for those units peaked around 250-275ms (Fig #). This observation suggests that raw neural activity is of secondary importance in network communications – by the time firing rate has peaked, causal measures are decreasing. In support of this interpretation, our analysis of 'task-insensitive' units finds significant causality components even in the absence of large firing rate changes. Future work should follow up on this observation to determine whether information conveyed by causality measures is similar to information that can be decoded from analysis of unit activity.

More generally, our analytic approach suggests a novel means by which the interactions of networked regions in the brain might be mapped. A clear shortcoming of our approach is that, due to computational demands, we were only able to analyze a bare fraction of the neurons available. Despite this drawback, however, we were able to observe 'interesting' patterns within the frontostriatal network that are broadly consistent with findings reported in the literature. This results suggests that our analytic approach might provide a new view of network interactions at

the level of individual units, and that continued refinement of the approach can be expected to yield even more insight into the function of neural networks.

Materials and Methods

Experimental animals. Data was collected from two adult, 9 and 7-year-old, male rhesus monkeys (Macaca mulatta) following procedures described in5. All animal care and experimental protocols were approved by the York University Council on Animal Care and were in accordance with the Canadian Council on Animal Care guidelines.

Behavioral paradigm. Monkeys performed a feature-based reversal learning task that required covert attention to one of two stimuli based on the reward associated with the color of the stimuli. Which stimulus color was rewarded remained identical for ≥30 trials and reversed without explicit cue. The reward reversal required monkeys to utilize trial outcomes to adjust to the new color-reward rule. Details of the task have been described before5. Each trial started when subjects foveated a central cue. After 0.5-0.9 sec, two black and white gratings appeared. After another 0.4 sec., the stimuli either began to move within their aperture in opposite directions (up-/downwards) or were colored with opposite colors (red/green or blue/yellow). After another 0.5-0.9 sec, they gained the color when the first feature was motion, or they gained motion when the first feature had been color. After 0.4-0.1 sec, the stimuli could transiently dim. The dimming occurred either in both stimuli simultaneously, or separated in time by 0.55 sec. Dimming represented the go-cue to make a saccade in the direction of the motion when it occurred in the stimulus with the reward associated color. The dimming acted as a no-go cue when it occurred in the stimulus with the non-rewarded color. A saccadic response was only rewarded when it was made in the direction of motion of the stimulus with the rewarded color. Motion direction and location of the individual colors were randomized within a block. Thus, the only feature predictive of reward within a block was color. Color-reward associations were constant for a minimum of 30 trials. Block changes occurred when 90% performance was reached over the last 12 trials, or 100 trials were completed without reaching criterion. The block change was uncued. Rewards were deterministic.

Electrophysiology. Extra-cellular recordings were made with 1–12 tungsten electrodes (impedance 1.2–2.2 MOhm, FHC, Bowdoinham, ME) in anterior cingulate cortex (ACC; area 24), prefrontal cortex (LPFC; area 46, 8, 8a), or anterior striatum (STR; caudate nucleus (CD), and ventral striatum (VS)) through a rectangular recording chambers (20 by 25 mm) implanted over the right hemisphere (Supplementary Fig. 1). Electrodes were lowered daily through guide tubes using software-controlled precision micro-drives (NAN Instruments Ltd., Israel and Neuronitek, Ontario, Canada). Data amplification, filtering, and acquisition were done with a multichannel acquisition system (Neuralynx). Spiking activity was obtained following a 300–8000 Hz passband filter and further amplification and digitization at 40 kHz sampling rate. Sorting and isolation of single unit activity was performed offline with Plexon Offline Sorter, based on analysis of the first two principal components of the spike waveforms. Experiments were performed in a custom-made sound attenuating isolation chamber. Monkeys sat in a custom-made primate chair viewing visual stimuli on a computer monitor running with a 60 Hz refresh rate. Eye positions were monitored using a video-based eye-tracking system (EyeLink, SRS Systems) calibrated prior to each experiment to a nine-point fixation pattern. Eye fixation was controlled within a 1.4°–2.0° radius

window. During the experiments, stimulus presentation, monitored eye positions, and reward delivery were controlled via MonkeyLogic (www.brown.edu/Research/monkeylogic/). Liquid reward was delivered by a custom-made, air-compression controlled, and mechanical valve system. Recording locations were aligned and plotted onto representative atlas slices (Calabrese et al., 2015).

Granger Causality Analyses. In order to examine causal influences amongst ACC, LPFC, and VS during correct behavioral trials, data from those trials was aligned on cue onset and reward onset periods, +/- 300ms. The activity for each unique electrode source was averaged over all trials to derive a mean activity profile across all recording sessions. There were a total of 3247 unique recording sites, distributed across ACC (1126), VS (1011) and LPFC (1110). In order to decrease the total number of pairwise granger causality analyses, we computed the standard deviation for each averaged activity time course. In each region, we selected only neurons ("task-sensitive" units) in the 97.5^{th} percentile for additional analysis, i.e., only those units that showed the greatest variation over each experimental epoch were part of our granger causality analyses. The rationale for this choice was twofold. First, units with high variance are likely to exhibit "interesting" activity profiles, likely as a result from participating in network interactions related to a task. Second, since Granger causality involves analysis of pairwise interactions, each additional unit included geometrically increases the total number of analyses to be conducted. We therefore limited our analyses to a small number of units from each region so that they could complete within a reasonable time frame. For the cue period, additional analyses were conducted on 28 ACC neurons, 24 VS neurons, and 28 LPFC neurons. For the reward period, 28 ACC neurons, 26 VS neurons, and 288 LPFC neurons were selected for additional analyses.

We compared causal influences observed for task-sensitive neurons during correct trials against causality estimates for neurons with around ½ the variance ("task-insensitive") as well as with task-sensitive neurons during error trials, by repeated our primary analyses. For these analyses, the neurons identified as having the highest variance for each region in the correct trials were used for analyzing causality in error trials, i.e., we did not repeat our neuron selection procedure using the error data. By using the same neurons for analysis of both correct and error trial data, we are able to compare differences in causality estimates that derive from behavioral performance. By using neurons with lower overall variability in their firing rates during correct trials, we are able to compare the downstream causal influence of task-sensitive neurons

Granger causality analyses were conducted using the Granger Causality toolbox for Matlab (https://www.dcs.warwick.ac.uk/~feng/causality.html). For each unique pairwise combination of neurons between two regions, a causal measure was estimated using a sliding 50ms window over the entire time course for those neurons, allowing us to estimate the causal influence of one neuron on another at 1ms intervals. The 50ms time window was selected based on previous analysis of the HER model (Alexander & Womelsdorf, 2018).

Cluster analysis. Following the causality estimation step, we conducted a kmeans cluster analysis on the resulting causality matrices (Fig #), where each row represents the pairwise combination of neurons from one region and another, and each column the estimated causality. The optimal number of clusters for the kmeans analysis was determined using the Matlab evalclusters function with a squared Euclidean distance and silhouette evaluation. To determine significance thresholds for causality estimation, we bootstrapped a causality distribution by selecting 50 points at random from the causality matrix for each region to construct an artificial time course for which we calculated causality. This procedure was repeated 100,000 times to derive the causality distribution. Significant differences in the net direction of causality for clusters recovered from our kmeans analyses were determined by conducting t-tests on the causality estimates for each neuron included in a cluster at each point in time.

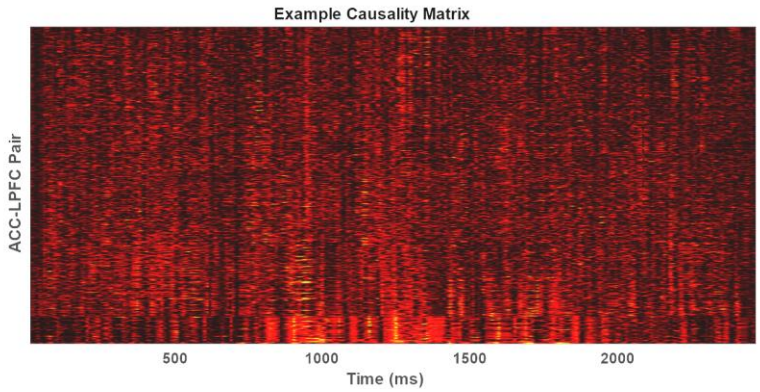

Figure 5 – Pairwise Granger Causality. Each row represents a single pair consisting of one neuron recorded from ACC and one neuron from LPFC during cue presentation (1250ms). Causality results were clustered using the kmeans clustering algorithm to identify distinct cluster components.

References

Akam, T., & Kullmann, D. M. (2014). Oscillatory multiplexing of population codes for selective communication in the mammalian brain. *Nature Reviews Neuroscience*, *15*(2), 111–122. https://doi.org/10.1038/nrn3668

Alexander WH, Brown JW (2015) Hierarchical Error Representation: A Computational Model of Anterior Cingulate and Dorsolateral Prefrontal Cortex. Neural Comput 27:2354-2410.

Alexander, W. H., & Brown, J. W. (2018). Frontal cortex function as derived from hierarchical predictive coding. *Scientific Reports*, *8*(1), 3843. https://doi.org/10.1038/s41598-018-21407-9

Alexander, H.A., and Womelsdorf, T. (2018). Interactions of medial and lateral prefrontal cortex in hierarchical predictive coding. 1-24. bioRxiv. doi:https://doi.org/10.1101/439927.

Antzoulatos EG, Miller EK. Increases in functional connectivity between prefrontal cortex and striatum during category learning. *Neuron* **83**, 216-225 (2014).

Arikuni, T., Sako, H., Murata, A. (1994) Ipsilateral connections of the anterior cingulate cortex with the frontal and medial temporal cortices in the macaque monkey. Neurosci Res 21:19-39.

Averbeck BB, Lehman J, Jacobson M, Haber SN (2014) Estimates of projection overlap and zones of convergence within frontal-striatal circuits. J Neurosci 34:9497-9505.

Badre D, Frank MJ (2012) Mechanisms of hierarchical reinforcement learning in cortico-striatal circuits 2: evidence from fMRI. Cereb Cortex 22:527-536.

Calabrese E, Badea A, Coe CL, Lubach GR, Shi Y, Styner MA, Johnson GA (2015) A diffusion tensor MRI atlas of the postmortem rhesus macaque brain. Neuroimage 117:408-416.

DeFelipe, J., & Fariñas, I. (1992). The pyramidal neuron of the cerebral cortex: Morphological and chemical characteristics of the synaptic inputs. *Progress in Neurobiology*, *39*(6), 563–607. https://doi.org/10.1016/0301-0082(92)90015-7

den Ouden, H. E. M. den, Daunizeau, J., Roiser, J., Friston, K. J., & Stephan, K. E. (2010). Striatal Prediction Error Modulates Cortical Coupling. *Journal of Neuroscience*, *30*(9), 3210–3219. https://doi.org/10.1523/JNEUROSCI.4458-09.2010

Frank MJ, Badre D (2012) Mechanisms of hierarchical reinforcement learning in corticostriatal circuits 1: computational analysis. Cereb Cortex 22:509-526.

Fries P. Rhythms for Cognition: Communication through Coherence. Neuron 88, 220-235 (2015).

Hahn G, Bujan AF, Fregnac Y, Aertsen A, Kumar A. Communication through resonance in spiking neuronal networks. PLoS Comput Biol 10, e1003811 (2014).

Hahn G, Ponce-Alvarez A, Deco G, Aertsen A, Kumar A. Portraits of communication in neuronal networks. Nat Rev Neurosci 20, 117-127 (2019).

Kayser, C., Montemurro, M. A., Logothetis, N. K., & Panzeri, S. (2009). Spike-Phase Coding Boosts and Stabilizes Information Carried by Spatial and Temporal Spike Patterns. *Neuron*, *61*(4), 597–608. https://doi.org/10.1016/j.neuron.2009.01.008

Leong YC, Radulescu A, Daniel R, DeWoskin V, Niv Y (2017) Dynamic Interaction between Reinforcement Learning and Attention in Multidimensional Environments. Neuron 93:451-463.

Lipsman N, Kaping D, Westendorff S, Lozano AM, Womelsdorf T. (2014) Beta coherence within human ventromedial prefrontal cortex precedes affective value-based choices. NeuroImage. 85(2): 769-778.

Lu, M.T., Preston, J.B., Strick, P.L. (1994) Interconnections between the prefrontal cortex and the premotor areas in the frontal lobe. J Comp Neurol 341:375-392.

Lundqvist M, Herman P, Warden MR, Brincat SL, Miller EK. Gamma and beta bursts during working memory readout suggest roles in its volitional control. Nat Commun 9, 394 (2018).

Luczak A, McNaughton BL, Harris KD. Packet-based communication in the cortex. Nat Rev Neurosci 16, 745-755 (2015).

Marco-Pallares, J., Cucurell, D., Cunillera, T., García, R., Andrés-Pueyo, A., Münte, T. F., & Rodríguez-Fornells, A. (2008). Human oscillatory activity associated to reward processing in a gambling task. *Neuropsychologia*, *46*(1), 241–248. https://doi.org/10.1016/j.neuropsychologia.2007.07.016

Markov, N., Misery, P., Falchier, A., Lamy, C., Vezoli, J., Quilodran, R., Gariel, M., Giroud, P., Ercsey-Ravasz, M., Pilaz, L., et al., 2011. Weight consis- tency specifies regularities of macaque cortical networks. Cerebral cortex 21, 1254–1272.

Markov, N.T., Vezoli, J., Chameau, P., Falchier, A., Quilodran, R., Huissoud, C., Lamy, C., Misery, P., Giroud, P., Ullman, S., et al., 2014. Anatomy of hierarchy: Feedforward and feedback pathways in macaque visual cortex. Journal of Comparative Neurology 522, 225–259.

Medalla, M., and Barbas, H. (2009). Synapses with inhibitory neurons differentiate anterior cingulate from dorsolateral prefrontal pathways associated with cognitive control. Neuron 61, 609-620.

Medalla, M., Gilman, J.P., Wang, J.Y., and Luebke, J.I. (2017). Strength and Diversity of Inhibitory Signaling Differentiates Primate Anterior Cingulate from Lateral Prefrontal Cortex. J Neurosci 37, 4717-4734.

Morecraft, R.J., Stilwell-Morecraft, K.S., Cipolloni, P.B., Ge, J., McNeal, D.W., Pandya, D.N. (2012) Cytoarchitecture and cortical connections of the anterior cingulate and adjacent somatomotor fields in the rhesus monkey. Brain Res Bull 87:457-4997.

Nácher V, Hassani, SA, Womelsdorf T (2019) Asymmetric effective connectivity between primate anterior cingulate and lateral prefrontal cortex revealed by electrical microstimulation. Brain Structure and Function. 224 (2), 779-793.

Oemisch M, Westendorff S, Everling S, Womelsdorf T (2015) Inter-areal spiketrain correlations of anterior cingulate and dorsal prefrontal cortex during attention shifts. Journal of Neuroscience 35(38):13076-89.

Oemisch M, Westendorff S, Azimi M, Hassani SA, Ardid S, Tiesinga P, Womelsdorf T (2019) Feature-specific prediction errors and surprise across macaque fronto-striatal circuits. Nat Commun 10:176.

O'Reilly, R. C., & Frank, M. J. (2006). Making working memory work: A computational model of learning in the prefrontal cortex and basal ganglia. *Neural Comput*, *18*, 283–328.

Palmigiano A, Geisel T, Wolf F, Battaglia D. Flexible information routing by transient synchrony. Nat Neurosci 20, 1014-1022 (2017).

Parr, T., & Friston, K. J. (2017). Working memory, attention, and salience in active inference. *Scientific Reports*, *7*(1), 14678. https://doi.org/10.1038/s41598-017-15249-0

Qiao S, Sedillo JI, Brown KA, Ferrentino B, Pesaran B (2020) A Causal Network Analysis of Neuromodulation in the Mood Processing Network. Neuron.

Rao, R. P. N., & Ballard, D. H. (1999). Predictive coding in the visual cortex: A functional interpretation of some extra-classical receptive-field effects. *Nature Neuroscience*, *2*(1), 79–87. https://doi.org/10.1038/4580

Rothe, M., Quilodran, R., Sallet, J., and Procyk, E. (2011). Coordination of high gamma activity in anterior cingulate and lateral prefrontal cortical areas during adaptation. The Journal of neuroscience: the official journal of the Society for Neuroscience 31, 11110-11117.

Sawaguchi, T., & Goldman-Rakic, P. S. (1991). D1 dopamine receptors in prefrontal cortex: Involvement in working memory. *Science*, *251*(4996), 947–950. https://doi.org/10.1126/science.1825731

Schneider, M., Dann, B., Sheshadri, S., Scherberger, H., & Vinck, M. (2020). A general theory of coherence between brain areas. bioRxiv: https://doi.org/10.1101/2020.06.17.156190.

Shin H, Law R, Tsutsui S, Moore CI, Jones SR. The rate of transient beta frequency events predicts behavior across tasks and species. Elife 6, (2017).

Voloh B, Valiante TA, Everling S, Womelsdorf T (2015) Theta gamma coordination between anterior cingulate and prefrontal cortex indexes correct attention shifts. PNAS, Proceedings National Academy of Science, USA. 112(27):8457-62.

Voloh B, Womelsdorf T (2018) Cell-type specific burst firing interacts with theta and beta activity in prefrontal cortex during attention states. Cerebral Cortex. 28: 4348-4364.

Voloh B, Oemisch M, Womelsdorf T (2020). Phase of Firing Coding of Learning Variables across Prefrontal Cortex, Anterior Cingulate and Striatum during Feature Learning. Nature Communications. https://doi.org/10.1038/s41467-020-18435-3

Voloh B, Valiante TA, Everling S, Womelsdorf T (2015) Theta gamma coordination between anterior cingulate and prefrontal cortex indexes correct attention shifts. PNAS, Proceedings National Academy of Science, USA. 112(27):8457-62

Wang, W., Viswanathan, S., Lee, T., & Grafton, S. T. (2016). Coupling between Theta Oscillations and Cognitive Control Network during Cross-Modal Visual and Auditory Attention: Supramodal vs Modality-Specific Mechanisms. *PLOS ONE*, *11*(7), e0158465. https://doi.org/10.1371/journal.pone.0158465

Womelsdorf T, et al. Modulation of neuronal interactions through neuronal synchronization. Science 316, 1609-1612 (2007).

Womelsdorf, T., Ardid, S., Everling, S., Valiante, T.A. (2014) Burst firing synchronizes prefrontal and anterior cingulate cortex during attentional control. Curr Biol 24:2613-2621.